Publ. Astron. Inst. ASCR 92, 1–14 (2004)

FOTEL 4 – User's guide

P. Hadrava

Astronomical Institute, Academy of Sciences of the Czech Republic,
251 65 Ondřejov, Czech Republic
e-mail: had@sunstel.asu.cas.cz
http://www.asu.cas.cz/˜had/fotel.html

FOTEL 4 is a FORTRAN code for separate or simultaneous solving of light curves, radial-velocity curves, visual (interferometric) measurements and eclipse timing of binary and/or triple stellar systems. The underlying physical assumptions, numerical methods and practical use of the code are described in this document.

Keywords: Binary stars – eclipsing, light-curves solution

Contents

1 Introduction **2**

2 Physical model **2**
2.1 Orbital motion . . . 2
2.2 Changes of light . . . 4
2.2.1 Shape of stars in Roche model . . . 4
2.2.2 Radiation in the approximation of triaxial ellipsoids . . . 5

3 Numerical methods **7**
3.1 Solution of elements . . . 7
3.2 Errors and correlations of elements . . . 10

4 User's manual **11**
4.1 Implementation of the code . . . 11
4.2 Main control keys . . . 11
4.3 Data format . . . 12
4.4 Dataset parameters . . . 12
4.5 Element parameters . . . 13
4.6 Output . . . 13

References **13**

A Combination of different solutions **14**

1 Introduction

The synthesis of the phase-dependent light and spectral changes of eclipsing binaries includes many physically interesting problems, the solution of which requires much larger effort and more computations than models of simple plane-parallel atmospheres. However, to be able to compare results of such theories with real observations, it is necessary to know basic physical parameters of the observed binary. These can be estimated using a program based on a rather simple analytical model. The need of these parameters, as well as practical needs of interpretations of photometric observations led to the development of FORTRAN code named FOTEL for solving of **phot**ometric **el**ements. This code is a supplement to the set of programs (e.g. the SPEL for the solution of the **sp**ectroscopic **el**ements, but also the programs for searching for period etc. and recently also KOREL for spectra disentangling[1]) developed at the Ondřejov observatory for data processing.

Some of the orbital elements and physical or geometrical parameters of a binary system are well defined by light curves (e.g. inclination i), while others can also be determined from radial velocities (RV-hereafter; some of the parameters are defined much better by RVs – e.g. the eccentricity e or the mass ratio q). It is therefore convenient to solve simultaneously for photometric and spectroscopic elements (Wilson 1979). For this reason FOTEL enables the separate or simultaneous solution of light- and RV-curves of binary stars. In this sense, FOTEL is a generalization of SPEL and it involves and extends its possibilities. SPEL can be faster in cases of simple binary orbits, it can also be used to estimate a zero order approximation for systems with some secular changes of orbital elements, if the observational data are divided e.g. by seasons. However, owing to its greater versatility, FOTEL can provide a direct fit more easily in such complicated cases.

The version FOTEL 3 of the code developed around 1990 can handle eccentric orbits of binaries including a possible third component (taking into account the corresponding light-time effect). Later versions can include into the solution also radial velocities of the third component. The solution of light-curves is based on an approximation of three-axial ellipsoids which proved to be viable even in the case of nearly contact binaries.[2] FOTEL 3 includes also a preliminary version enabling to deal with the generalized Roche geometry of components and physics of their atmospheres as described by Hadrava (1987b, 1988). However, this part of the code is not still reliably debugged and for this reason its description is skipped here. The simplicity of the three-axial aproximation allows to fit a large amount of individual data-points. FOTEL enables to find and eliminate some systematic differences between sets of observational data from different instruments and methods of data reduction. This is why it has been requested by some colleagues to give the code and its description at public disposal even in the unfinished version.

The present version FOTEL 4 enriches the possibilities of FOTEL 3 by simultaneous solution of visual orbits of the close pair and timing of light-curve minima caused by the eclipses (in addition to the solution of complete light-curves and RV-curves). The first generalisation is done because of the progress of instrumentation, especially in interferometry, which enabled to fill the gap between the wide visual and close spectroscopic binaries. The second one is to profit from the older observations of poorer quality, which, however, are useful for determination of the precise value of orbital period (cf. Hadrava 2005).

The PC-version of FOTEL and a brief manual to it are presented in this document, which is an updated version of manual available in electronic form (Hadrava 1991). However, note that the code is still under development and is being updated from time to time. Necessarily, the same is true for this description (and partly also for the built-in *Help* which, however, is not frequently used). The users of FOTEL are thus asked to pay an attention to the date of their release of both the code and the manual, and to verify if some new versions are accessible on web (http://www.asu.cas.cz/~had/fotel.html). The source files of the code and examples of the input data can be downloaded by authorized users.[3]

2 Physical model

2.1 Orbital motion

The primary and the secondary star are supposed to move in Keplerian orbits

$$r_{1,2} = \frac{a_{1,2}(1-e^2)}{1+e\cos v} , \tag{1}$$

[1] The code KOREL uses the technique of Fourier decomposition developed from the method of radial-velocity determination by cross-**cor**relation and the experience from determination of orbital **el**ements in FOTEL (cf. Hadrava 2004: "KOREL – User's guide" in this volume).

[2] Kallrath and Milone (1999) give a comprehensive review of different codes for light-curve solution and the corresponding physics. Several codes are based on assumption of Roche geometry. The difference between the Roche geometry and its three-axial approximation is appreciable mainly in the vicinity of the inner Lagrangian point L_1 for components nearly filling their Roche lobe. However, the region of L_1-point is hidden during the eclipses, which dominate the light-curve solution. Moreover, the assumptions of Roche geometry are anyway violated for components close to their Roche lobe.

[3] The IP-address of computer(s) for which the access is requested should be sent (e.g. via the author's e-mail address given above in heading) to register and to get on the list of authorized users.

$$v = 2\mathrm{arctan}\left(\sqrt{\frac{1+e}{1-e}}\mathrm{tg}\frac{E}{2}\right) , \quad (2)$$

$$M = E - e\sin E \quad (3)$$

around the center of gravity of this pair, which itself can be in a similar motion around the common center of mass with a distant third star (the orbital elements corresponding to the third companion will be identified by dashed symbols). Secular changes of period P, periastron longitude ω and semimajor axes $a_{1,2}$ can be included into the calculation. The mean anomaly M is therefore calculated from the heliocentric time t of observation as

$$M = 2\pi\frac{\tau}{P_0}\left(1 - \frac{\tau}{2P_0}\left(\dot{P}_0 + k\frac{\tau}{P_0}\right)\right) , \quad (4)$$

where

$$\tau \equiv t - t_0 - \Delta t , \quad (5)$$

t_0 is the epoch of the reference periastron passage (which is taken also as the origin of phases), Δt is the correction for light-time effect

$$\Delta t = \frac{P' K_{1+2}}{2\pi c}(1-e'^2)^{3/2}\frac{\sin(\omega'+v')}{1+e'\cos(v')} , \quad (6)$$

where K_{1+2} is the semiaplitude of the center of mass of the subsystem of stars No. 1 and 2 with respect to the total center of mass including the star No. 3, c is the speed of light, and

$$k = \frac{1}{3}(P_0\ddot{P}_0 - 2\dot{P}_0^2) . \quad (7)$$

The instantaneous period $P(t)$ is given by

$$P^{-1}(t) = \frac{1}{2\pi}\frac{dM}{dt} = \frac{1}{P_0}\left(1 - \frac{\tau}{P_0}\left(\dot{P}_0 + \frac{3k\tau}{2P_0}\right)\right) \quad (8)$$

and its change

$$\dot{P}(t) = -\frac{P^2(t)}{2\pi}\frac{d^2M}{dt^2} = \frac{P^2(t)}{P_0^2}\left(\dot{P}_0 + 3k\frac{\tau}{P_0}\right) . \quad (9)$$

Note, that it is customary to express the timing of minima (to investigate their O–C) by the relation inverse to Eq. (4)

$$t = t_0 + P_0\left(\frac{M}{2\pi}\right) + \frac{P_0\dot{P}_0}{2}\left(\frac{M}{2\pi}\right)^2 + k'\left(\frac{M}{2\pi}\right)^3 , \quad (10)$$

where

$$k' = \frac{P_0}{6}(P_0\ddot{P}_0 + \dot{P}_0^2) = \frac{P_0}{2}(k + \dot{P}_0^2) . \quad (11)$$

Neither the period ($P = 2\pi\frac{dt}{dM}$), nor its time derivative ($\dot{P} = \frac{4\pi^2}{P}\frac{d^2t}{dM^2}$) are polynomial functions of time in this approximation. An alternative formula

$$M = 4\pi\frac{\tau}{P_0}\left(1 + \sqrt{1 + 2\dot{P}_0\frac{\tau}{P_0}}\right)^{-1} , \quad (12)$$

to Eq. (4) can be chosen by setting $key(7) = 1$ (cf. Section 4.2). This formula is asserted by Petr Harmanec because it holds constant increase of period $\Delta P = \dot{P}P = \dot{P}_0 P_0$.

The secular changes of ω, K-velocities $K_{1,2}$ as well as those of other parameters are taken as linearly varying with time

$$\omega(t) = \omega_0 + \dot{\omega}_0\tau \qquad \text{etc.} \quad (13)$$

The observed radial velocities of the primary or secondary component are supposed to correspond to the motion of centers of both stars

$$RV_{1,2} = K_{1,2}[\cos(\omega+v) + e\,\cos(\omega)] + +K_{1+2}[\cos(\omega'+v') + e'\cos(\omega')] + \gamma , \quad (14)$$

where the semiamplitudes $K_{1,2}$ are related with the mass ratio $q = M_2/M_1$ of the components and with the above used orbital elements by

$$K_1 = -qK_2 = \frac{2\pi a_1 \sin i}{P\sqrt{1-e^2}} , \quad (15)$$

i is the inclination of the orbit. The radial velocity of the third star is

$$RV_3 = -K_3[\cos(\omega'+v') + e'\cos(\omega')] + \gamma . \quad (16)$$

Note, that while K_2 and K_{1+2} are converged in ratio with K_1, the amplitude K_3 is converged in its absolute value (cf. Tab. I on p. 7).

The projection $r_\perp$ on the sky of the instantaneous distance $r = r_1 + r_2$ between the components of the close pair is given by

$$r_\perp^2 = \left(\frac{a(1-e^2)}{1+e\cos v}\right)^2\left[1 - \sin^2(\omega+v)\sin^2 i\right] , \quad (17)$$

and the position angle ϕ by

$$\mathrm{tg}\,\phi = \cos\,i\;\mathrm{tg}(\omega+v) . \quad (18)$$

The angular distance of the stars is fitted in logarithmic scale and the position angle is fitted as another independent variable (despite they are usually measured simultaneously). The phases and epochs of primary and secondary photometric minima due to eclipses are calculated by minimization of expression (17)

$$0 = \frac{dr_\perp^2}{dv} = \frac{2a^2(1-e^2)^2\sin^2 i}{(1+e\cos v)^3}\left[e\sin v\,\mathrm{ctg}^2 i - \cos(\omega+v)\left(\sin(\omega+v) + e\sin\omega\right)\right] . \quad (19)$$

For $i = \pi/2$ the minima are identical with conjunctions of the stars during their apparent motion in the direction of the line of nodes,

$$\cos(\omega+v) = 0 , \quad (20)$$

however, for slightly smaller inclinations they can differ from the conjunctions due to the relative motion of stars perpendicularly to the line of nodes

$$\cos(\omega+\upsilon) \simeq \frac{e\cos\omega\cos^2 i}{\sin^2 i + e\sigma\sin\omega} \, , \tag{21}$$

where $\sigma = \mathrm{sign}(\sin(\omega+\upsilon))$ distinguishes between the primary and secondary minimum. This solution, which is of the second order in $\cos^2 i$, gives generally better results for all cases in which the eclipses can occur ($i \simeq \pi/2$, e arbitrary) than the analogous approximation (VI.9-22) obtained by Kopal (1959) using the expansion up to the second order in e (even if the sign of the second-order term is corrected in his formula). The times and phases of reference primary and secondary minimum, together with those of RV$_{max}$, RV$_{min}$ and conjunctions are also given in the output.

2.2 Changes of light

In general, the shapes of both stars can vary in the course of the orbital motion with non-zero eccentricity or for an oblique rotation. Consequently, the conditions for calculation of the proper shape and the reflected radiation of both stellar discs, as well as the geometry of their eclipse should be calculated separately for each point in the light-curve. Due to the varying tidal force, a binary component can not be in exact hydrostatic equilibrium if it is not co-rotating with the orbital motion, i.e. if the synchronism or co-planarity of the equator with the orbit or the zero eccentricity are violated. Actually, distortions of the shape of star leading to the tidal synchronization take place in these cases. Exactly speaking, even if all these conditions are satisfied, the hydrostatic equilibrium is incompatible with the radiative equilibrium in the illuminated and/or gravitationally darkened atmosphere (Hadrava 1987b, 1988). None the less, the shape of the star can be approximated by equipotentials of an effective potential.[4] Because the calculation of the shapes of the stars and their corresponding radiation is numerically relatively exhaustive task, it is possible in FOTEL 4 to choose between the approximation of the stellar shapes by triaxial ellipsoids (which is faster and usually satisfactory) or by the Roche equipotentials (which is physically more convincing). The corresponding models are described in this Section.

Even if the quasi-hydrostatic assumption of equipotential shapes of stars is accepted, the choice of the proper equipotential attributed to the stellar surface is an open question. The estimate of variations of the stellar inner structure due to the varying tidal force and its consequences for the surface layer has been studied by Hadrava (1986). The result includes the assumption of constant volume used by Wilson (1979) as a special case for a particular value ($\gamma = 1.25$, which dosn't seem to be much plausible) of the polytropic index of subphotospheric layers (the mantle). The polytropic approximation is thus used in FOTEL as a compromise between the traditionally accepted but physically non-acceptable approximations and a desirable but still non-existing and probably numerically very complicated physical model. A similar argumentation can be led e.g. for the problem of gravity darkening (Hadrava 1988).

[4]Such a generalization of Roche model for nonsynchronism was suggested by Kopal (1956), who used wrong potential. Correct one was found by Plavec (1958), see also Limber (1963) and Wilson (1979) for the explanation.

2.2.1 Shape of stars in Roche model

Following Wilson (1979), the effective potential in a component (e.g. the primary) of the binary is given by

$$\begin{aligned}\Phi(\vec{x}) \;=\; & -\frac{\Omega^2 a^2}{1+q}\left[\frac{a}{x} + \frac{qa}{|\vec{x}-\vec{r}|} - \frac{qa}{r} - \frac{qa}{r^2}x_r + \right. \\ & \left. + \frac{(1+q)Q^2}{2a^2}(x^2 - x_Q^2)\right] \, ,\end{aligned} \tag{22}$$

where $\vec{x}$ is the radius-vector from the centre of the star ($x \equiv |\vec{x}|$), $\Omega = 2\pi/P$ is the mean orbital angular frequency, a is the semimajor axis, $q = M_2/M_1$ is the mass ratio, $\vec{r}$ is the instantaneous position of the secondary ($r \equiv |\vec{r}|$), Q is the synchronization index of the star, i.e. the ratio of sidereal rotational and orbital frequency, x_r and x_Q are the projections of $\vec{x}$ on $\vec{i}_r \equiv \vec{r}/r$ (the direction of $\vec{r}$) and on $\vec{i}_Q$ (the direction of the rotational axis), respectively. The rotational axis is not necessarily perpendicular to the orbital plane. Its orientation is defined by polar distance θ_Q and the longitude ϕ_Q (measured in the direction of orbital motion) in spherical coordinates with the pole perpendicular to the orbital plane and the main meridian given by $\vec{r}$ at the time t_0 of the priastron passage. The rotational axis is supposed to hold its orientation with respect to the inertial frame in the course of the orbital motion or to precess with the rate $\dot{\phi}_Q$. The instantaneous angle $\theta(t)$ between $\vec{i}_Q$ and $\vec{i}_r$ is thus given by

$$\cos\theta = \sin\theta_Q\cos(\upsilon - \phi_Q + (\dot{\omega}_0 - \dot{\phi}_Q)\tau) \, . \tag{23}$$

The potential (22) possesses the mirror symmetry with respect to the plane defined by $\vec{i}_Q$ and $\vec{i}_r$. The net of spherical coordinates with the main meridian in this plane and the pole in direction $\vec{i}_r$ (where there can be the singularity in L_1-point in the classical case) is thus used to describe the stellar surface.

The potential (22) can be decomposed into a part

$$\bar{\Phi}(x) = -\frac{\Omega^2 a^2}{1+q}\left[\frac{a}{x} + \frac{(1+q)Q^2}{3a^2}x^2\right] \, , \tag{24}$$

which is spherically symmetric with respect to the centre of the star, and the asymmetrical part

$$\begin{aligned}\tilde{\Phi}(\vec{x}) &= \Phi - \bar{\Phi} = -\frac{\Omega^2 a^2}{1+q}\left[\frac{qa}{|\vec{x}-\vec{r}|} - \frac{qa}{r} - \frac{qa}{r^2}x_r + \right. \\ &\left. + \frac{(1+q)Q^2}{6a^2}(x^2 - 3x_Q^2)\right] = \\ &= -\frac{\Omega^2 a^2}{1+q}\left[\frac{qa}{2r^3}(3x_r^2 - x^2) + \right. \\ &\left. + \frac{(1+q)Q^2}{6a^2}(x^2 - 3x_Q^2) + \frac{qa}{r}o((\frac{x}{r})^3)\right] \end{aligned} \quad (25)$$

which vanishes if averaged over the solid angle measured from the centre of the star

$$\langle\tilde{\Phi}\rangle \equiv \int_{x=\mathrm{const.}} \tilde{\Phi}\frac{d^2\omega}{4\pi} = 0 \ . \quad (26)$$

Obviously, the third term in the bracket on the right hand side of Eq. (22), which is constant at a given moment, compensates the variation of the potential caused by the companion star in the centre of the binary. We will use the potential (24) to define the effective radius R of the star as the radius, at which

$$\bar{\Phi}(R) \equiv -\frac{\Omega^2 a^2}{1+q}\left[\frac{a}{R} + \frac{(1+q)Q^2}{3a^2}R^2\right] = \Phi_0 \ , \quad (27)$$

where Φ_0 is the value of the total potential (22) at the surface. If the equation $\Phi(\vec{x}) = \Phi_0$ (where the left and right hand side are given by (22) and (27), respectively) is solved with respect to the square of the denominator x of the first term in Eq. (22) and the higher order terms in x/a or R/a are neglected like in Eq. (25), we can get the equation

$$x^2 + \alpha(3x_r^2 - x^2) + \beta(3x_Q^2 - x^2) = R^2 \quad (28)$$

of the triaxial ellipsoid approximating the shape of the primary star, where

$$\alpha = -\frac{qR^3}{r^3} \quad \text{and} \quad \beta = \frac{(1+q)Q^2R^3}{3a^3} \ . \quad (29)$$

The corresponding semi-major axes are

$$\begin{aligned}A_{1,2} &= R\left[1 - \frac{\alpha+\beta}{4} \pm \right. \\ &\left. \pm\frac{3}{4}\sqrt{\alpha^2 + (4\cos\theta - 2)\alpha\beta + \beta^2}\right]\end{aligned} \quad (30)$$

in the plane $(\vec{i}_Q, \vec{i}_r)$ and

$$A_3 = R\left[1 + \frac{\alpha+\beta}{2}\right] \quad (31)$$

perpendicularly to this plane. Obviously, $A_1A_2A_3 \simeq R^3$, hence the volume of a sphere with the effective radius R (defined to fit the potential on the surface) is equal (in the first approximation) to the volume of the triaxial ellipsoid.

2.2.2 Radiation in the approximation of triaxial ellipsoids

In this model the shapes of stars are approximated by triaxial ellipsoids with the semiaxes

$$A = D\left[1 + \frac{R^3}{q}\left(-\frac{2}{r^3} - (1+q)Q^2\right)\right]^{-1/2} \quad (32)$$

$$B = D\left[1 + \frac{R^3}{q}\left(\frac{1}{r^3} - (1+q)Q^2\right)\right]^{-1/2} \quad (33)$$

$$C = D\left[1 + \frac{R^3}{qr^3}\right]^{-1/2} \ , \quad (34)$$

in directions toward the companion, perpendicular to it in the orbital plane and perpendicular to the orbital plane, respectively. Here

$$D = R\left[1 - \frac{2}{3}\frac{1+q}{q}Q^2R^3\right]^{1/2} \ , \quad (35)$$

r is the instantaneous distance between centers of the stars, Q is the synchronization index, i.e. the ratio of rotational and orbital frequency, and R is effective radius $\left(\simeq (ABC)^{1/3}\right)$. R varies according to

$$\frac{q}{2R^2} + \frac{2}{3}(1+q)Q^2R + \frac{4\kappa-5}{\kappa-1}\frac{1}{2qr^2} = const., \quad (36)$$

where κ is the polytropic index of the star ($p \sim \rho^\kappa$; note, that R is constant for κ=1.25) – cf. Hadrava (1987). The effective radii $R_{1,2}$ of components at periastron are the elements of the light curve (i.e. a free parameters to be given in the input or found by the solution). The zero-points of light-curves are adjusted to luminosities of uneclipsed discs with these radii.

The instantaneous luminosity $L_{\lambda,j}$ of the j^{th} star is taken proportional to the area of its apparent disc

$$L_{\lambda,j} = \left(\frac{R_{a,j}}{R_j}\right)^2 10^{-.4m_{\lambda,j}} \ , \quad (37)$$

where the apparent radius R_a is given by

$$\begin{aligned}R_a^2 &= \left[A^2B^2\cos^2 i + (B^2 + \right. \\ &\left. +(A^2 - B^2)\cos^2(\omega+v))C^2\sin^2 i\right]^{1/2} \ .\end{aligned} \quad (38)$$

The 3[rd] star is assumed to be spherical, consequently $L_{\lambda,3} = 10^{-.4m_{\lambda,3}}$, or $L_{\lambda,3} = 0$ for $R_3 = 0$. Provided that the temperature T_j of the j-th star (j=1, 2, 3) is set $\leq$0, the corresponding colour magnitudes $m_{\lambda,j}$ are taken as independent variables and the value of the wavelength λ has no influence on them. If, however, $T_j > 0$, the colour magnitudes are calculated to correspond to the black-body radiation,

$$m_{\lambda,j} = -2.5\log\left(R_{a,j}^2\frac{B_\lambda(T_j)}{B_\lambda(T_0)}\right) + \Delta m_j \ , \quad (39)$$

where T_0 is the temperature of a reference star (e.g. the comparison star if the data from differential photometry are reduced, or a star of spectral type A0, T_0=10 000 K, which is included in the code as a standard). In the former case, it is customary to separate the data from various spectral bands into different *Datasets*, while in the later case it is advantageous to merge them into a common *Dataset* to make the temperature responsible for the differences between their zero-levels. Note, that in any case, only the differences between magnitudes of the stars ($m_{\lambda,j}$ or Δm_j) are defined by the light curves, while their absolute value and the zero-level are linearly dependent. It is thus recommended to fix the magnitudes of one star (e.g. primary) equal to a chosen value (e.g. zero or the absolute magnitudes corresponding to its spectral type).

The reflection of the light from the secondary star on the surface of the primary is included according to the formula by Formiggini and Leibowitz (1990) corrected by Hadrava (1992b)

$$L_{1,2} = \frac{k_{\lambda,1}L_{\lambda,2}}{3-u}\frac{B_1C_1B_2C_2}{4\pi r^2 R_2^2}\left[\frac{3u\pi}{4}(1+\cos\alpha)^2 + +4(1-u)(\sin\alpha+(\pi-\alpha)\cos\alpha)\right] , \quad (40)$$

where u is the limb-darkening coefficient and

$$\alpha = \arccos[\sin i \sin(\omega + \upsilon)] \quad (41)$$

is the angle between the line of sight and the direction toward the companion. The effective monochromatic reflection albedo $k_{\lambda,j}$ can be fixed or converged as a free parameter of the light curve, if the temperature of the particular star is set $\leq$0. If this temperature (e.g. for the primary) is 0 and the temperature of the second star is $\neq$0, the albedo is calculated from

$$k_{\lambda,1} = \frac{hcT_2^4}{4k\lambda T_1^5}\frac{\exp(\frac{hc}{k\lambda T_1})(\exp(\frac{hc}{k\lambda|T_2|})-1)}{(\exp(\frac{hc}{k\lambda T_1})-1)^2} . \quad (42)$$

For the reflection on the secondary ($j = 2$), the change of indices 1 and 2 and $\alpha \to \pi - \alpha$ must be done in the above formulas.

In general, the reflection reduces the limb darkening, which could be taken into account according to Vaz and Nordlund (1985). However, a treatment of such small effects would be justified only after including a more realistic model of the atmosphere, hence the limb darkening of the reflected light is supposed to be equal to the limb darkening of the proper radiation of the star

$$\Delta I(\cos\psi) = \Delta I_1.(1-u+u\cos\psi) \quad (43)$$

($u = u_{\lambda,j}$) in the present version of FOTEL.

The geometry of the eclipses is simplified to occultation of two circular discs with apparent radii R_a and linear limb darkening u. The luminosity ΔL obscured during the eclipse of the primary thus reads

$$\begin{aligned} \Delta L &= 0 && \text{for } r_\perp > R_{a,1}+R_{a,2} \\ &= L_{\lambda,1} && \text{for } r_\perp + R_{a,1} < R_{a,2} \\ &= \int_0^{R_{a,1}^2} I(\mu)\varphi(\rho)d\rho^2 , && (44) \end{aligned}$$

where

$$I(\mu) = \frac{3(L_{\lambda,1}+L_{1,2})}{\pi R_{a,1}^2(3-u)}(1-u+\mu u) , \quad (45)$$

$$\mu = \sqrt{1-\rho^2/R_{a,1}^2} , \quad (46)$$

and

$$\begin{aligned} \varphi(\rho) &= 0 && \text{for } \rho < r_\perp - R_{a,2} \\ &= 0 && \text{for } \rho > r_\perp + R_{a,2} \\ &= \pi && \text{for } \rho < R_{a,2} - r_\perp \\ &= \arccos\frac{\rho^2+r_\perp^2-R_{a,2}^2}{2\rho r_\perp} . && (47) \end{aligned}$$

We have assumed here that the reflected light is eclipsed in the same way as the radiation of the star itself. The integral in Eq. (44) for the last case of Eq. (47) is calculated numerically. For the secondary minimum, the indices 1 and 2 have to be interchanged.

To enable a search for periodic changes in O–C (arising e.g. from a periodicity of the third light, or from the rotation of a spotted – but not occulted) component – a periodic term

$$\delta m_\lambda(t) = \delta m_{0,\lambda}\sin(2\pi\frac{t-t_0'}{P'}) \quad (48)$$

is included to the total magnitude whenever the period P' is nonzero.

The resulting magnitude of the whole system thus reads

$$m_\lambda = -2.5\log(L_{\lambda,1}+L_{\lambda,2}+L_{\lambda,3}-\Delta L+L_{1,2}+ +L_{2,1}) + (t-t_0)\frac{dm_\lambda}{dt} + DA_\lambda + \delta m_\lambda , \quad (49)$$

where D is the reddening and A_λ extinction coefficient.

Gravity darkening and correlated gravity-limb darkening are to be included into a new version of FOTEL with exact Roche geometry. However, up to now, elements between No. 143 and 189 (cf. Tab. I) are not used in the present version of the code.

[5] The time unit can be arbitrary for the calulations, however, some physical values on output are correctly calculated only if this time unit is chosen days.

[6] The periastron longitude and its time derivative were given in radians in old versions of FOTEL. It is still calculated in radians internally, however, it is converted to degrees on input and output.

[7] Note that in versions up to FOTEL 3, the value of $\sin i$ was read at input instead of the inclination. The value of i is (equally as ω) calculated in radians internally, but read in degrees.

Table I. List of elements

n	E_n	E_{min}	E_{max}
1	P Orbital period [in an arbitrary time unit][5]	0	$+\infty$
2	t_0 Periastron epoch [time unit]		
3	e Eccentricity	0	1
4	ω Periastron longitude [deg][6]		
5	K_1 Amplitude of R.V. [km/s]		
6	$q = m_2/m_1$ mass ratio		
7	R_1 Radius [in units of semimajor axis]	0	$1 - E_3$
8	R_2 Radius [in units of semimajor axis]	0	$1 - E_3 - E_7$
9	i inclination [deg][7]		
10...19	$\delta m_{0,\lambda}$		
20...29	A_λ extinction coefficients	0	$+\infty$
30...39	$u_{\lambda,1}$ limb darkening of primary	0	1
40...49	$u_{\lambda,2}$ limb darkening of secondary	0	1
50	dP/dt		
51	P' Period of the 3rd star [time unit]	0	$+\infty$
52	t'_0 Periastron epoch of the 3rd star [time unit]		
53	e' Eccentricity of the 3rd star	0	1
54	ω' Periastron longitude of the 3rd star [deg][6]		
55	K_{1+2}/K_1		
56	$d\omega/dt$ [deg / time unit][6]		
57, 58	$\kappa_{1,2}$ Polytrop. index of 1st and 2nd star	1	$+\infty$
59	Q_1 Synchroniz. index of 1st star		
60...69	$k_{\lambda,1}$ Albedo of the primary		
70...79	$k_{\lambda,2}$ Albedo of the secondary		
80...89	dm_λ/dt Linear trend [in mag. per time unit]		
90	Q_2 Synchroniz. index of 2nd star.		
91...94	T_1, T_2, T_3, T_0 Temperatures [K]		
95	R_3 Radius [in units of close-pair semimajor axis]		
96...98	$\Delta m_{1,2,3}$ Corrections of magnitudes		
99	D Reddening	0	$+\infty$
100...109	λ Wavelengths [Å]		
110...119	$m_{\lambda,1}$ Colour magnitudes of the 1st star		
120...129	$m_{\lambda,2}$ Colour magnitudes of the 2nd star		
130...139	$m_{\lambda,3}$ Colour magnitudes of the 3rd star		
140	dK_1/dt		
141	$dK_2/dt - K_2/K_1 * dK_1/dt$		
142	$\frac{1}{3}(P_0\ddot{P}_0 - 2\dot{P}_0^2)$		
143...145	$\theta_{Q,1}$, $\phi_{Q,1}$, $\dot{\phi}_{Q,1}$ orientation of the 1st star rotation [radian]		
146...148	$\theta_{Q,2}$, $\phi_{Q,2}$, $\dot{\phi}_{Q,2}$ orientation of the 2nd star rotation [radian]		
150...159	gravity darkening of the 1st star		
160...169	gravity darkening of the 2nd star		
170...179	correlated darkening of the 1st star		
180...189	correlated darkening of the 2nd star		
190	K_3 [km/s]		

3 Numerical methods

3.1 Solution of elements

The solution of light- and/or RV- curves, as well as the fit of visual orbit or timing of minima is based on the minimization of the sum $\Sigma_{(O-C)^2}$ as a function of the elements. Here Σ means summation over all points

$$\Sigma(p) = \sum_I \frac{W_I}{K_{I0}^2} \sum_{i \in I} w_i \left[y_i - f(x_i, p)\right]^2 \ , \tag{50}$$

where x_i, y_i and w_i are the time, value and the weight of the i-th point in the *Input file*, respectively, f is the theoretical value at x_i corresponding to the appropriate *Type of variable* for the given values of parameters p. W_I is the common weight of the *Data set* Nr. I to which the i-th point belongs. This weight is reduced by the square of the coefficient K_{I0}, which is set equal to the initial value of K_1 for the *Data sets* containing RV's, or to 1 for *Data sets* with the colour magnitudes, distances, position angles or the timing. This normalization transforms the range of RV's to the order of unity comparable to the range of photometry given in magnitudes or the other quantities in their corresponding units to enable the summation of their contributions to Σ for the simultaneous solution. The influence of different types of data and their sets on the solution can be tuned by appropriate choice of W_I.

The minimization formally corresponds to the solution of the set of equations

$$\begin{aligned} 0 &= \frac{\partial \Sigma(p)}{\partial p_\alpha} = \qquad (51) \\ &= -2\sum_I \frac{W_I}{K_{I0}^2} \sum_{i\in I} w_i \left[y_i - f(x_i,p)\right] \frac{\partial f(x_i,p)}{\partial p_\alpha} \,. \end{aligned}$$

These equations reduce to a simple set

$$0 = \sum_I \frac{W_I}{K_{I0}^2} \sum_{i\in I} w_i \left[y_i - \sum_\beta p_\beta f_\beta(x_i) \right] f_\alpha(x_i) \qquad (52)$$

of linear equations in parameters p if f is a linear combination of p,

$$f(x_i,p) = \sum_\alpha p_\alpha f_\alpha(x_i) \,. \qquad (53)$$

This is indeed the case for radial velocities (see Eq. (14)), which can be rewritten for the simple motion as

$$\begin{aligned} RV &= [K\cos\omega]\cos\upsilon - [K\sin\omega]\sin\upsilon + \\ &\quad +[Ke\cos\omega + \gamma] \,, \qquad (54) \end{aligned}$$

(cf., e.g., van Paradijs et al., 1977). The elements γ, K and ω can be thus solved analytically if P, e and t_0 are either known or calculated numerically. The same is true for all γ's of different *Data sets*, for K_2 or K and ω of the third motion (provided that the non-linear influence of light-time effect is neglected). However, for the model of light curves, f is non-linear in both ω and the mass-ratio $q = m_2/m_1 = K_1/K_2$, as well as in most of the other parameters apart from the zero-points of the *Data sets*. We will thus assume

$$f(x_i,p) = p_I + K_i \bar{f}(x_i,\bar{p}) \,, \qquad (55)$$

where the parameter $K_i \equiv K_1$ will be calculated for the radial velocities as

$$K_1 = \frac{\sum_{I\ni \mathrm{RV}} W_I \left[\sum_{i\in I} w_i y_i \bar{f}_i - \frac{\sum_i w_i y_i \sum_i w_i \bar{f}_i}{\sum_i w_i}\right]}{\sum_{I\ni \mathrm{RV}} W_I \left[\sum_{i\in I} w_i \bar{f}_i^2 - \frac{(\sum_i w_i \bar{f}_i)^2}{\sum_i w_i}\right]} ,\qquad (56)$$

and it will be fixed $K_i \equiv 1$ for *Data sets* containing photometry, visual positions or timing. For all types of data apart of the timing (for which it is set equal to zero) the zero-points p_I of the *Data sets* are calculated as

$$p_I = \frac{\sum_{i\in I} w_i y_i - K_I \sum_i w_i \bar{f}_i}{\sum_{i\in I} w_i} \,, \qquad (57)$$

the contribution Σ_I of the I-th *Data sets* to the total sum as

$$\Sigma_I = \sum_{i\in I} w_i \left[y_i - p_I - K_I \bar{f}_i\right]^2 / K_{I0}^2 \,, \qquad (58)$$

and the mean error of the measurements in the I-th *Data set* reads

$$\Delta_I = \left\{ \sum_{i\in I} w_i \left[y_i - p_I - K_I \bar{f}_i\right]^2 / \sum_{i\in I} w_i \right\}^{1/2} \,. \qquad (59)$$

In these equations f_i is the abbreviation for $f(x_i,\bar{p})$, which now gives the theoretical magnitudes or theoretical RV's divided by K_1, $\bar{p}$ denotes all the other elements (which will be calculated numerically) apart of K_1 and zero-points p_I.

The minimization in non-linear parameters $\bar{p}$ is carried out using the simplex method as it has been described by Kallrath and Linnell (1987). The number of transformations of the simplex in each step is 10-times the number of elements being converged in the step (the linear parameters, which are calculated directly by least square method as described above are not included in this number). The maximum number of parameters allowed to converge in one step was limited to 10 in older versions of FOTEL and it is increased to 20 on request of some users. However, it is recommended to proceed with the solution carefully, allowing first to converge a few most crucial parameters and to improve the solution by converging the less important parameters only afterwards. The experience shows that additional parameters often result in shallow local minima and enable the simplex to fall in them before it can perceive the global behaviour of the minimized function.

Following Horn's numerical approach in SPEL, the values E_n of elements are transformed for the optimization by logarithmic transformation

$$\begin{aligned} p_n &= \ln\left(\frac{E_n - E_{min}}{E_{max} - E_n}\right) \quad \text{for } E_n \in (E_{min}, E_{max}) \\ &= \ln(E_n - E_{min}) \quad \text{for } E_{max} = +\infty, \qquad (60) \\ &= E_n \quad \text{for } E_{max} = +\infty,\ E_{min} = -\infty \end{aligned}$$

which maps the range of their physically meaningful values (E_{min}, E_{max}) into the infinite interval $(-\infty, +\infty)$ – see Tab. I.

The above explained transformation of variables enables to avoid meaningless solutions like those with

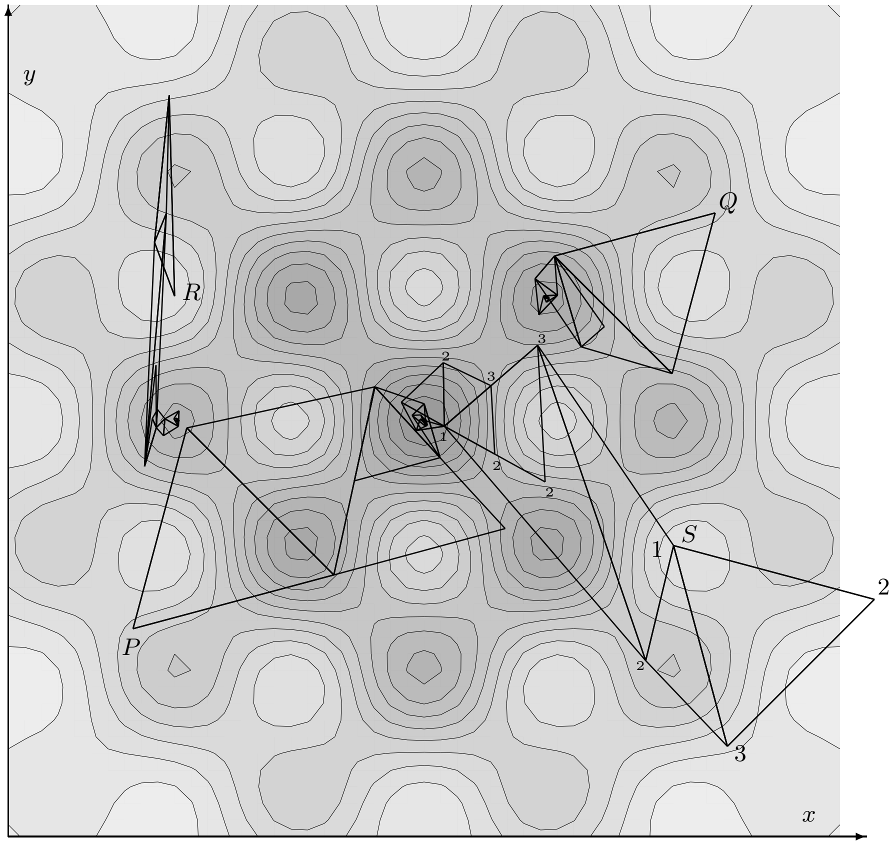

Fig. 1. Minimization of 2-dimensional function $-\exp(-x^2-y^2)(2+\cos(10x)\cos(10y))$ by simplex method. The simplex converges into the global minimum in the point (0,0) from initial points P and S, while for the initial point Q (which is symmetric with respect to P) it stops at a local minimum because of smaller values of initial steps. Similarly, simplex starting from point R (symmetric with S) falls into another local minimum in the direction of y-axis earlier than it can start to move in the x-direction for which the initial step was chosen too small. The points of the initial simplex at S are labeled by their numbers and their positions after the corresponding simplex oparations by small digits – cf. the protocol on the convergence listed in text. (Taken from Hadrava 2003b.)

negative luminosities or orbital eccentricity or with a sum of radii larger than the distance of components etc. Actually just these transformed parameters p are the independent variables in which $\Sigma_{(O-C)^2}$ is minimized. The initial steps of elements are multiplied by $\frac{dp}{dE}$ to obtain the steps of parameters. The values of p's are also displayed in the protocol on the convergence, an example of which follows.

```
 1 B 2 -.53203E+00  .10830E+01 -.42941E+00
 2 C 3 -.64052E+00  .72941E+00 -.78296E+00
 3 C 1 -.66915E+00  .60000E+00 -.30000E+00
 4 B 2 -.13512E+01  .53295E+00 -.57678E+00
 5 D 2 -.17099E+01  .29112E+00 -.14698E+00
 6 A 2 -.18449E+01  .16987E+00 -.79954E-01
 7 A 3 -.19105E+01  .16090E+00  .84454E-01
 8 B 2 -.21068E+01  .46160E-01  .13991E+00
 9 B 3 -.27563E+01 -.54781E-01  .44622E-01
 ...
19 B 2 -.30000E+01  .66453E-03 -.31106E-03
20 B 3 -.30000E+01 -.53478E-03 -.19750E-03
21   1 -.30000E+01  .35233E-03  .31267E-03
21   3 -.30000E+01 -.28705E-04  .16289E-04
```

Here the first column gives the sequential number of simplex operation, the second one gives its code (A means reflection, B contraction, C expansion and D shrinkage – cf. Kallrath and Linnell, 1987), the number of the worst point of the simplex is in the third one. Next follows the value of the sum $\Sigma_{(O-C)^2}$ and then its coordinates (i.e. the transformed values of the converged parameters in the order in which they were introduced in *element-parameters*). Last two rows of the protocol without the code of operation give the number and value of the worst point followed by the final steps of parameters (which are used as initial in the following step) and number, value and parameters of the best point at the end of the run of simplex minimization. Values of steps and elements are then transformed back to their physically meaningful form and given on output. This protocol enables to check the procedure of simplex minimization. First, the values of $\Sigma_{(O-C)^2}$ should decrease with the only possible exception for operation D. If this sum reaches a constant value well before the end of the procedure, the result can be accepted. In the opposite case, it should be continued by a new run. The presence of number 1 in the third column indicates, that the initial value has been improved by the procedure (number 1 need not to appear in a case of D-operation). If $\Sigma_{(O-C)^2}$ is much higher in the first row than for the first improvement of the initial value, the initial step of the corresponding parameter[8] was too high and should be decreased not to waste steps and to give a chance to other parameters to improve their values. The user should be aware that the simplex method cannot guarantee to find the global minimum. The success depends on the reasonable choice of the converged parameters, their initial estimates and initial values of steps.

3.2 Errors and correlations of elements

The errors of the elements found by the above described method are given by the depth and the shape of the function $\Sigma_{(O-C)^2}(p)$ in the vicinity of the particular solution (i.e. a local minimum) in the p-space. These characteristics of Σ are further determined by the errors of the input values y_i, by their distribution in time (x_i) as well as by the nature of the solved problem – e.g. the epoch of periastron passage and the longitude of periastron are not well defined for orbits of small eccentricities (they are highly correlated), each of them has large error (even if the second one is fixed) if the data available cover only the extremes of RV or, certainly, if they have large scatter.

If we suppose $p = p(y)$ to be the formal solution of Eq. (51), then the perturbation δp_α of a particular element caused by a small error δy_i of any input value y_i is given by the relations

$$0 = \frac{\partial^2 \Sigma(p)}{\partial p_\alpha \partial p_\beta} \delta p_\alpha - 2 \frac{W_I}{K_{I0}^2} w_i \frac{\partial f_i}{\partial p_\beta} \delta y_i \; . \tag{61}$$

Assuming the errors δy_i to be statistically independent, we can calculate the statistical average of the correlation of errors of parameters

$$\langle \delta p_\alpha \delta p_\gamma \rangle = \Sigma^{-1}_{\alpha\beta} \Sigma^{-1}_{\gamma\delta} \sum_I \frac{W_I^2}{K_{I0}^4} \sum_{i \in I} w_i^2 \frac{\partial f_i}{\partial p_\beta} \frac{\partial f_i}{\partial p_\delta} \langle \delta y_i^2 \rangle \; , \tag{62}$$

where Σ^{-1} is the inverse matrix to the matrix of the second-order derivatives

$$\Sigma_{\alpha\beta} \equiv \frac{1}{2} \frac{\partial^2 \Sigma(p)}{\partial p_\alpha \partial p_\beta} = \tag{63}$$
$$= \sum_I \frac{W_I}{K_{I0}^2} \sum_{i \in I} w_i \left\{ \frac{\partial f_i}{\partial p_\alpha} \frac{\partial f_i}{\partial p_\beta} - [y_i - f_i] \frac{\partial^2 f_i}{\partial p_\alpha \partial p_\beta} \right\} \; ,$$

which, in the first approximation, describes the shape of the function Σ in the vicinity of its minimum.

Following the assumption (55), this matrix can be simplified for the linear parameters p_I and K as

$$\Sigma_{IJ} \equiv \frac{1}{2} \frac{\partial^2 \Sigma(p)}{\partial p_I \partial p_J} = \delta_{IJ} \frac{W_I}{K_{I0}^2} \sum_i w_i \tag{64}$$

$$\Sigma_{IK} \equiv \frac{1}{2} \frac{\partial^2 \Sigma(p)}{\partial p_I \partial K} = \frac{W_I}{K_{I0}^2} \sum_i w_i \bar{f}_i \tag{65}$$

$$\Sigma_{KK} \equiv \frac{1}{2} \frac{\partial^2 \Sigma(p)}{\partial K^2} = \sum_I \frac{W_I}{K_{I0}^2} \sum_i w_i \bar{f}_i^2 \; , \tag{66}$$

and for the mixed derivatives in linear and non-linear $(\bar{p}_\alpha)$ parameters as

$$\Sigma_{I\alpha} \equiv \frac{1}{2} \frac{\partial^2 \Sigma(p)}{\partial p_I \partial \bar{p}_\alpha} = \frac{W_I}{K_{I0}} \sum_i w_i \frac{\partial \bar{f}_i}{\partial \bar{p}_\alpha} \tag{67}$$

$$\Sigma_{K\alpha} \equiv \frac{1}{2} \frac{\partial^2 \Sigma(p)}{\partial K \partial \bar{p}_\alpha} = \sum_I \frac{W_I}{K_{I0}} \sum_i w_i \bar{f}_i \frac{\partial \bar{f}_i}{\partial \bar{p}_\alpha} \; , \tag{68}$$

while the derivatives in both non-linear parameters must be calculated according to Eq. (50). The term containing the 2[nd]-order derivatives of f_i in this equation is neglected in the present version of FOTEL. Because the derivatives of f with respect to non-linear parameters cannot be in general simply expressed as functions of p, they are calculated numerically as finite differences with steps in p determined by the instantaneous extension of the simplex.

Usually, we have no information on the errors δy_i in advance. Note, that these errors can be much higher than the instrumental ones if there a physical process takes place, which is not included in our theoretical model (e.g. a flickering for the photometry). Consequently, we will assume this error to be the same for all data in the same *Dataset* equal to the value Δ_I given by Eq. (59). The correlation (62) thus reads

$$\langle \delta p_\alpha \delta p_\gamma \rangle = C_{\alpha\beta} \equiv \tag{69}$$
$$\equiv \Sigma^{-1}_{\alpha\beta} \Sigma^{-1}_{\gamma\delta} \sum_I \frac{W_I^2}{K_{I0}^4} \Delta_I^2 \sum_{i \in I} w_i^2 \frac{\partial f_i}{\partial p_\beta} \frac{\partial f_i}{\partial p_\delta} \; .$$

This assumption is not exact e.g. for the photometry, which has lower S/N-ratio in a deep minimum, or provided we solve a phase-curve, where the probable error of each normal point can be obtained from the scatter of the original data. In such cases an improvement can be achieved by a proper choice of the

[8]In our example, which corresponds to the evolution of simplex starting from the point S in Fig. 1, the highest initial simplex point has number 2 (however, its value is not much higher due to asymptotic flatness of the minimized function and because the initial steps are chosen properly), what corresponds to the first converged parameter x.

weights $w_i \sim (\delta y_i)^{-2}$. A similar choice of weights of *Datasets*, $W_I \sim (\Delta_I)^{-2}$, is recommended to optimize the use of information stored in the data. The matrix C is computed with respect to the transformed parameters p and then it is multiplied by the Jacobian $\frac{\partial E}{\partial p}$ of the transformation (60) to give the standard deviations of elements and/or zero-points of *Datasets* $\sqrt{C_{\alpha\alpha}}$ and their correlations $C_{\alpha\beta}/\sqrt{C_{\alpha\alpha}C_{\beta\beta}}$ on output.

The complete covariance matrix consisting of errors of parameters together with their correlations should be given to enable to judge the level of consistency of solutions obtained from different source data (as argued in Hadrava 2003a). A simple code named COMBI performing such a calculation is available (see the Appendix A below).

4 User's manual

4.1 Implementation of the code

The code FOTEL is written in the language FORTRAN 77. It has been developed and debugged originally on computers of the type of IBM 370, later mostly using MS-Fortran for PC. However, it can also be successfully compiled with other compilers (e.g. g77 under UNIX or LINUX) and used on different computers (e.g. on workstations of the type of SUN or on VAXes). Some minor changes of the code can be necessary for compilation with a particular compiler, e.g. the command `$LARGE` must be switched on or off if the MS-Fortran is or is not used. Starting from version of 2004, dimensions of arrays limiting the capacity of the code can be adjusted as a parameter in the file FOTELPAR.F (which has to be accessible to the compiler together with the main source code FOTEL.FOR).

Apart of the compiled code, the file FOTEL.IN must be accessible for the running of the code and the accessibility of the file FOTEL.HLP is necessary to enable the use of built-in help mode. Other files with input- (i.e. the initial estimates of parameters and the measurements) and output- (i.e. the resulting elements and the O–C) data can be defined by the user. Examples of the file FOTEL.IN and the corresponding input and output files are available on the web home-page of FOTEL.

4.2 Main control keys

The code starts by reading so called *Main control keys*, $key(i)|_{i=1}^{10}$ (by `FORMAT(16I5)`) from the file FOTEL.IN.

$key(1)$ can switch the code into the interactive mode (if it is given =0), in which it behaves like the versions of FOTEL till January 1992, or to the automatic mode (if it is given =5).[9] In the later case the subsequent information is read from FOTEL.IN instead of from the keyboard (the breaks of output and corresponding instructions for continuation are omitted in this case if the output-file for parameters is opened). The interactive mode continues at the top-level menu, where the keys $key(i)|_{i=2}^{6}$ (i.e. *Inpar*, *Outpar*, *Input*, *Output* and *Echo*) have to be given again (`FORMAT(*,*)`). The first four of them define whether the corresponding Input/Output files are required (positive value) or not (zero value).

If $key(2) \equiv Inpar \in \langle 1, 99\rangle$, the name of file with the initial values of elements (see **Element parameters**) is read.[10] This file is closed immediately after the elements are read. $Inpar > 99$ switches the run into the Help-mode of the code (this is useful in the interactive mode only), $Inpar < 0$ terminates the calculation.

If $key(3) \equiv Outpar > 0$, the principal results will be stored in a file.[11] $Outpar > 1$ sets a higher level of the output, in which the protocol about the convergence and a table of values (after the convergence) of all elements are written into the output file.

$key(4) \equiv Input > 0$ indicates the input of observational data from a file[12] (see **Data format**). If $Input = 0$, the previously entered data are used. If $Input < 0$, a synthetic curve is generated (i.e. 50 points with time-step =1/50 of the time-unit), the $Type\ of\ variable = \mathrm{abs}(Input)$.

$key(5) \equiv Output > 0$ causes the residual $O - C$ of individual data-points, their phases with respect to both periods etc. to be written to a file.[13]

$key(6) \equiv Echo > 0$ causes that all data read from the keyboard are displayed on the screen. If $Echo > 1$ then the data from Input-file are also displayed.

$key(7) = 1$ switches on the calculation of $\dot{P}$ according to Eq. (12).

$key(8) > 0$ switches on the automatic end of convergence (its value gives the number of digits of $\Sigma(O-C)$ taken into account).

$key(9) = 0$ switches on the triaxial ellipsoid approximation to the shape of binary components. If $key(9) > 0$ in FOTEL 4 (release starting from July 1993), it gives the number of points in latitude and $2key(9) - 2$ gives the number points in longitude on the component surfaces. It thus has to be equal to 3 at least and, due to limited array dimensions, equal to 13 at maximum.

$key(10) > 0$ increases the weight of photometric

[9] The automatic mode is mostly used in practice.

[10] It means it is the second record of the file FOTEL.IN in the automatic mode.

[11] The user is asked in the interactive mode to specify its name for the first time of its use, or it has to be given in the subsequent record of the file FOTEL.IN in the automatic mode.

[12] Its name is to be given as before.

[13] Its name is to be given again.

observational points $2^{key(10)}\times$ to hit the solution of light-curves with narrow minima poorly covered by observations and noisy maxima.

4.3 Data format

The data to be fitted must be prepared in an *Input-file*, the name of which is typed on the request of FOTEL in its interactive mode, or it is typed in the file FOTEL.IN. This file is supposed to contain one comment record (`FORMAT(1X,79A1)`) followed by records,[14] each one containing single data point in the following structure:
$Time$, $Value$, $Sign(*)$, $Weight(1.0)$, End, $Dataset(1)$, $Type\ of\ variable(3)$, $Text$
written by `FORMAT(2F10.4,1A1,F8.2,I1,2I5,40A1)`. The defaults are given in brackets.

$Time$ can be given in arbitrary units (e.g., in periods for phase curves), but the light-time effect as well as some quantities on output are calculated assuming that the time-unit is the day (usually the $Time$ is given by Julian date).

$Value$ gives the magnitude, radial velocity, angular distance and position angle according to the appropriate $Type\ of\ var.$ (cf. Tab. II) observed at the given $Time$. Radial velocities are to be given in km/s to yield the correct light-time effect etc. (as mentioned above for the $Time$). $O-C$ is normalized per the initial value of K_1 for RV's and per magnitude for light curves to be comparable in the procedure of simultaneous solution.

An alphabetic character $Sign$ is ignored by FOTEL, but it is hold for the compatibility of the data with other Ondřejov programs for graphic output.

$Weight$ gives relative weight of the point within the $Data-set$.

$End > 0$ marks the last record to be taken into account.

$Dataset \in \langle 1, 30\rangle$ denotes to which set of data (see **Dataset parameters**) the particular point belongs. This allows the user to treat the possible zero-point shifts introduced by different spectrographs or photometer or photometric band passes. *Datasets* of the individual points must be chosen reasonably to separate radial velocities from magnitudes as well as different colours, provided the colour correction is not specified.

[14]The maximum number of these records taken into account is given by the parameter **npnt** in the source-file FOTELPAR.F.

[15]The angular distance can be given on input in arbitrary units (typically in seconds of arc), but it is transformed to logaritmic scale for the fitting of the orbital parameters, so that the zero-point of the corresponding *Dataset* gives the relation between the distance of the binary and the unit of input data.

[16]The position angle is to be given in degrees on input, but it is transformed into radians for the fitting.

[17]The $Value$ is ignored and it is set equal to the $Time$ for type of variable equal to 16. Zero levels of *Datasets* containing timing are fixed to be =0.

Table II. Types of variables

1	Radial velocity of the primary [km/s]
2	Radial velocity of the secondary [km/s]
3–12	Magnitudes in different colour bands
13	Radial velocity of the third star [km/s]
14	Angular distance between the primary and the secondary[15]
15	Position angle[16]
16	Timing of minima[17]

$Type\ of\ variable$ distinguishes whether the observed $Value$ at the point is radial velocity of primary or secondary component ($Type = 1, 2$ – in agreement with SPEL), or if it is magnitude in a particular filter ($Type = 3, ..., 12$). The first two *Datasets* and the minimal and maximal $Value$ appearing for the points of the particular $Type$ in the file (and vice versa the first two $Types$ for each *Dataset*) appear on the output.

This sequence of comment-record and data-records can be repeated, provided the previous one is ended by $End > 0$.

4.4 Dataset parameters

All data in the file can be divided into several (30 at maximum) sets called *Datasets* to enable to calculate their different zero-points (e.g. γ-velocities for data originating from different spectrographs like in SPEL, or systematic shifts for differential photometry obtained with respect to different comparison stars). These zero-levels of *Datasets* are calculated by direct least-square algorithm before the simplex method is used. They cannot be fixed and they are not included in the limit of 10 parameters which can be simultaneously converged in one step. The contributions of separate *Data sets* to the total sum are given at the beginning and the end of each step and each of them can be multiplied by an arbitrarily chosen common weight of the *Data set* (standard value =1) to diminish or to strengthen its influence on the solution. Any *Data sets* distinguished in the *Input file* can be merged during the calculation if their common zero-point is required.

These changes of weight or identity of *Datasets* are controlled by *Dataset parameters*, which must be typed from the keyboard (in free format) in order $Number\ of\ dataset$ (1...30), $New\ number$ (to which the dataset is to be merged or ≤ 0 if it has to be unchanged) and the $Weight$ of the dataset, i.e. coefficient by which the $Sum\ contribution$ $(O-C)^2$ and Sum of weights of individual measurements is to be multiplied. Input of $Dataset\ parameters$ is terminated if *Number of dataset*=0 is typed. New check sum is then displayed and possibility of new change of *Dataset parameters* is offered. The convergence is started if no change is typed. If *Number of dataset* < 0, then the calculation is returned to input of **Main control keys** at top-level menu.

4.5 Element parameters

Elements of the binary are numbered as listed in the Tab. I on p. 7. These elements can be read either from *Inpar*-file (see **Main control keys**), or from the keyboard. In the former case the *Inpar*-file must consist of records containing the *Number of element*, its *Value* and value of its initial *Step* (in free format). This file is read immediately after the nonzero *Inpar*-key is given at **Main control keys**. In the later case of the input from the keyboard the *Number of elements* is followed by three integer keys (> 0 means yes, ≤ 0 means no):
Converge – determining if the element is to be converged,
Change of value – if the value has to be changed and
Change of step – if the step has to be changed.
Further there must be two real numbers – new *Value* and *Step* – which are taken into account only in the cases of positive corresponding keys *Ch. val.* and *Ch. step*. Input of Element parameters is terminated if the *Nr. of element* ≤ 0 is typed (note, that it must be followed by 5 dummy parameters).

4.6 Output

The output is sent from FOTEL to the screen and, if the corresponding keys *Outpar* and *Output* are on, also to output files for parameters and for the individual points of data, resp. Meaning of some of the output data is obvious; here will be commented the opposite cases.

During the iteration, the protocol on the simplex convergence is shown on the screen enabling to estimate its progress. For each step of the simplex operation there is its number within the loop followed by its code A, B, C or D (cf. p. 9) and the number of the worst point of the simplex. At the beginning 1 corresponds to the initial estimate of parameters and $1+n$ to the point with dominant change of the n-th (by its order) parameter converged by simplex. The first improvement of the initial estimate thus takes place only when Nr. 1 appears; it may be helpful to decrease the initial step of the parameter which gives the first worst point, if the improvement occurs too late or not at all. In the next column, there is the value of the sum in the worst point. It should decrease in the course of the convergence (the shrinkage of simplex, i.e. D, may cause also a small increase) and a constant value indicates the simplex being at a local minimum. Next there are values of parameters at the worst point transformed according to Tab. I on p. 7. At the end of the loop both the worst and the best point are indicated, the first one with the actual (transformed) values of the steps and the second one with the transformed values of parameters.

In the output of parameters, the errors and cross-correlation coefficients of all converged parameters are followed by a table of all parameters listed in Tab. I.

Some of the basic parameters are then printed with higher precision and also some of their consequences are calculated. Note, that some of them are reasonable only if the input data are in standard units (time in days and RV's in km/s). Finally, for each period in question, there printed a histogram of the distribution of data points in bins wide 0.05 in phase, to give an estimate how the curve is covered.

In the output of data there is printed a table, where in the first column is the time of observation, in the second one is the input value corrected for the zero point of its data set, in the third column is the phase with respect to the period of the close orbit (corrected for the light-time effect and the secular change of period) and next is O–C. If the period of wide orbit is non-zero, the corresponding phase is printed in the fifth column (note that in older versions this column was printed ever as the fourth one) and for velocities there are finally printed in two additional columns also residuals after the subtraction of the motion in the close and wide orbit, resp.

Acknowledgement

This work has been supported by project K1048102 of the Academy of Sciences of the Czech Republic.

References

Formiggini L., Leibowitz E. M.: 1990, A&A 227, 121
Hadrava P.: 1987a, Hvar Obs. Bull. 10, 1
Hadrava P.: 1987b, Publ. Astron. Inst. CS. Ac. Sci. No. 70, 263
Hadrava P.: 1988, Publ. des Astrophys. Obs. zu Potsdam Nr. 114, Band 33, Heft 2, 11
Hadrava P.: 1990, Contrib. Astron. Obs. Skal. Pl. 20, 23
Hadrava P.: 1991, "FOTEL – User's guide" (electronic document), Astron. Inst. ČSAV
Hadrava P.: 1992a, A&A 256, 519
Hadrava P.: 1992b, A&A 257, 218
Hadrava P.: 1998, Hvar Obs. Bull. 22, 75
Hadrava P.: 2003a, "Spectroscopy of binary stars", in: *New directions for close binary studies: The royal road to stars*, O. Demircan, E. Budding (eds.), Publ. COMU Ap. Research Center, Vol. 3, pp. 84-90
Hadrava P.: 2003b, Scripta astronomica 10, 71
Hadrava P.: 2004, Publ. Astron. Inst. ASCR 92, 15
Hadrava P.: 2005, Astrophys. & Sp. Sc. 296, 239

Kopal Z.: 1956, Annales d'Astrophysique 19, 298
Kopal Z.: 1959, *Close Binary Systems*, Chapman & Hall, London
Kallrath J., Linnell A. P.: 1987, ApJ 313, 346
Kallrath J., Milone E. F.: 1999, *Eclipsing Binary Stars – Modeling and Analysis*, Springer-Verlag, New York, Berlin
Limber D. N.: 1963, ApJ 138, 1111
Paradijs J. A. van et al.: 1977, A&AS 30, 195
Plavec M.: 1958, Mém. Soc. R. Sc. Liége (4) 20, 411
Vaz L. P. R., Nordlund Å.: 1985, A&A 147, 281
Wilson R. E.: 1979, ApJ 234, 1054

A Combination of different solutions

Let us have k solutions (labeled by capital subscript A) of a fit in an n-dimensional space of parameters $\mathbf{p} \equiv \{p^i|_{i=1}^n\}$, each one characterized by a distribution $f_A(\mathbf{p})$ of probability of particular values of $\mathbf{p}$. The probability that $\mathbf{p}$ satisfies all these solutions is simply the product

$$f(\mathbf{p}) = \prod_{A=1}^{k} f_A(\mathbf{p}) \; . \tag{70}$$

The combination of the solutions can be defined as maximum of this function, which characterizes its distribution.

Suppose all the solutions have the normal distributions

$$\begin{aligned} f_A(\mathbf{p}) &= N(\mathbf{p};\mathbf{p}_A,\sigma_A) \equiv (2\pi)^{-\frac{n}{2}}|\sigma_A|^{-\frac{1}{2}} \\ &\quad . \exp\left(-\frac{1}{2}(\mathbf{p}-\mathbf{p}_A)^{\mathrm{T}}\sigma_A^{-1}(\mathbf{p}-\mathbf{p}_A)\right) \end{aligned} \tag{71}$$

with maxima at values $\mathbf{p} = \mathbf{p}_A$ and the covariance matrices σ_A. The distribution of their combination is then also a normal distribution

$$f_0(\mathbf{p}) = N(\mathbf{p};\mathbf{p}_0,\sigma_0) \tag{72}$$

where

$$\sigma_0^{-1} = \sum_{A=1}^{k} \sigma_A^{-1} \; , \tag{73}$$

$$p_0 = \sigma_0 \sum_{A=1}^{k} \sigma_A^{-1} p_A \; . \tag{74}$$

The probability of this combined solution can be taken as

$$\begin{aligned} P_0 &\equiv \prod_{A=1}^{k} \frac{f_A(\mathbf{p}_0)}{f_A(\mathbf{p}_A)} = \\ &= \exp\left(\frac{1}{2}\mathbf{p}_0^{\mathrm{T}}\sigma_0^{-1}\mathbf{p}_0 - \frac{1}{2}\sum_{A=1}^{k}\mathbf{p}_A^{\mathrm{T}}\sigma_A^{-1}\mathbf{p}_A\right) \; . \end{aligned} \tag{75}$$

The values of P_0, $\mathbf{p}_0$ and σ_0 can be calculated from the output of errors and correlation coefficients from FOTEL using the code COMBI.

The input of this code has to be in file COMBI.IN and its format is shown in the following example:

```
2
1 0 0. 1.
3 0 0. 0.
1 1 1. 1.
3 3 1. 1.
3 1 0.9999 -0.9999
```

The first line gives the number (k) of solutions to be combined, subsequent lines give the values of parameters, errors and correlations for these solutions in last k columns. The first two columns i, j (integer) distinguish the parameter components to which the correlations refer, or the error of the component if $i = j$, or the value of the parameter, if $j = 0$. These lines can be given in an arbitrary order.

The output of this code (for the above example) has the form

```
Calculation of consistency of 2 solutions
                              with  2 parameters:
1    param.  1      .000000E+00  .100000E+01
1  1 error=  1  1   .100000E+01  .100000E+01
2    param.  3      .000000E+00  .000000E+00
2  2 error=  3  3   .100000E+01  .100000E+01
2  1 corel.  3  1   .999900E+00 -.999900E+00
Probability=exp(-.250000E+00)= .778801E+00
Common solution:
1    param.  1      .500000E+00
1  1 error=  1  1   .999975E-02
2    param.  3      .499950E+00
2  2 error=  3  3   .999975E-02
2  1 corel.  3  1   .000000E+00
```

The input values are repeated at the top (the indices in the left columns correspond to the order of components in the input, the indices right to the explanatory abbreviation are the original names of components on input). Then the probability is given according to Eq. (75). Finally, the combined solution is given in the same format.

Note at this example, that despite both solutions give the same value (0.0) of the second component (named 3), their combination gives a different value (nearly 0.5) due to the large (nearly 1) correlation of the first and anticorrelation of the second solution.

It should be also noted, that the quadratic approximation used in Eq. (71) is applicable in a small vicinity of the solution only. It means that, for instance, two solutions of periodic light curve of RV-curve related to different epochs of periastron can be found mutually inconsistent within a small error of this parameter, despite they are actually identical.